

University of Louisville

ThinkIR: The University of Louisville's Institutional Repository

Electronic Theses and Dissertations

5-2013

Biomodeling of pancreatic tumor mass.

Justin Lee Howell
University of Louisville

Follow this and additional works at: <https://ir.library.louisville.edu/etd>

Recommended Citation

Howell, Justin Lee, "Biomodeling of pancreatic tumor mass." (2013). *Electronic Theses and Dissertations*. Paper 643.
<https://doi.org/10.18297/etd/643>

This Master's Thesis is brought to you for free and open access by ThinkIR: The University of Louisville's Institutional Repository. It has been accepted for inclusion in Electronic Theses and Dissertations by an authorized administrator of ThinkIR: The University of Louisville's Institutional Repository. This title appears here courtesy of the author, who has retained all other copyrights. For more information, please contact thinkir@louisville.edu.

Biomodeling of Pancreatic Tumor Mass

By

Justin Lee Howell
B.S., University of Louisville, 2012

A Thesis
Submitted to the Faculty of the
University of Louisville
J. B. Speed School of Engineering
as Partial Fulfillment of the Requirements
for the Professional Degree

MASTER OF ENGINEERING

Department of Bioengineering

BIOMODELING OF PANCREATIC CANCER CELLS

Submitted by: _____
Justin Lee Howell

Thesis Approved on

_____ 4/17/13 _____
(Date)

by the Following Reading and Examination Committee:

Hermann B. Fricobes, Thesis Director

Andrea S. Gobin

Gail W. Depuy

Acknowledgments:

Special thanks was credited to Dr. Hermann Frieboes, who acted as my advisor for the project and thesis, Dr. Lacey McNally, who provided a biological facility to gather data for my thesis, and Justin Huang, who aided my lab work for my thesis.

ABSTRACT

Pancreatic adenocarcinoma is the fourth leading cause of cancer death in the United States. It is identified by its rapid, invasive progression with a profound resistance to treatments such as chemotherapy. Unfortunately, there is a lack of information on how to effectively inhibit and control the rapid growth of pancreatic tumors, as well as limited information for diagnostics. With current methods, pancreatic cancer will continue to prevail as a leading cause of cancer death. We propose to study the complexity of pancreatic tumors with a systematic and analytical approach. Cancer is an abnormal growth of tissue caused by uncontrolled cell division. Observing the growth of these cells would prove to have a good basis to monitor the growth of a tumor. Here we create a 3-D simulation of tumor growth through mathematical modeling, using data from pancreatic cells grown *in vitro*. Using 3-D models will help to understand pancreatic tumors at cellular and molecular levels.

The project aims to observe realistic growth of the tumor, accomplished from growing tumor cells on a monolayer in order to find parameters for our 3D mathematical model. This method will prove more beneficial than testing only on a monolayer cell line. Although cell death and the toxicity of drug dosage can be tested using a cell monolayer alone, it does not meet the demands of testing drug

delivery in a realistic tumor environment that the mathematical model would provide. The monolayer lacks the dimensions that the drug would have to travel if it were delivered to a real *in vivo* tumor. A possible continuation of this project in the future could be to utilize the mathematical based approach to predict optimal therapy for the pancreatic tumor in order to develop models that can better test patient care for tumors. Computer modeling, another stepping stone through mathematical modeling, will possibly lead to testing the toxic effects of drugs on a 3-D model through computer modeling will aid in understanding the delivery of drugs throughout the tumor *in vivo*.

NOMENCLATURE

A	ratio of cell death to cell mitosis
G	ratio of cell mitosis to mechanical relaxation
L	diffusion length
R	radius of spheroid tumor
λ_M	mitosis rate
λ_D	cell death rate
λ_R	intrinsic relaxation rate
∇	del (vector differential)
u	cell velocity
λ_P	cell-proliferation rate
λ_A	apoptosis rate
b	measure of mitosis
n	concentration of cell substrate
Γ	rate at which nutrient is added
D	diffusion coefficient
λ_B	blood-tissue transfer rate of nutrient
n_B	concentration of nutrient in blood
B	measure of vascularization
μ	mobility of cell
P	oncotic pressure

TABLE OF CONTENTS

APPROVAL PAGE	iii.
ACKNOWLEDGEMENTS	iv.
ABSTRACT	v.
NOMENCLATURE	vii.
I. INTRODUCTION	1
II. MATERIALS AND METHODS	
A. Summary	2
B. Cell Culture	4
C. Trypan Blue Staining and Cell Counting	5
D. Mathematical Model Setup	5
III. DATA AND RESULTS	11
IV. DISCUSSION	13
V. REFERENCES	17

I. Introduction

Pancreatic adenocarcinoma is the fourth leading cause of cancer death in the United States. Out of the population in the U.S., it was estimated that 37,000 men and women will die from pancreatic cancer in 2012 alone (statistics from National Cancer Institute). Even when the tumor was identified, there was only a 5% chance of survival [3]. This may lead to the fact that diagnostics fail to locate a pancreatic growth until it has grown sufficiently into a malignant tumor. A pancreatic tumor is identified by its rapid, invasive progression with a profound resistance to treatments such as chemotherapy. It goes unnoticed for months without notice due to its deep location, hidden by other organs. It may only present itself when it grows large enough and begins to push against surrounding tissue, such as intestine, bile ducts, and nervous system [7]. Even then, the initial diagnosis can be associated with other illnesses due to the tumor only presenting unspecific symptoms (i.e. nausea, difficult motor function). This leaves patients with a late stage of correct diagnosis and a smaller survival rate.

A problem, therefore, seems to be poor understanding of what occurs when a tumor becomes malignant. Diagnostics aimed specifically at pancreatic cancer have not advanced much. With the rapid growth of pancreatic cancer, diagnosticians need to know what stage a tumor has entered in order to quickly assess the proper treatment a patient requires. To this end, a link between tumor

stages and the rapid growth of pancreatic cancer would assist in finding the best course of action for a patient after diagnosis of the tumor.

The proposed project is to use mathematical models to represent tumor growth. Unlike observing growth of cancer through monolayers, this model would allow us to understand the more complex arrangement of tumor cells as they interact [1], [2]. This is a relatively new method for observing cancer growth. This provides a better way of studying cellular interactions and would represent an *in vivo* environment. It is believed that this will provide a guideline to identify when a tumor mass is benign or malignant [5].

II. Materials and Methods

A. Summary

The mathematical model for the tumor will represent a tumor mass that grows in an avascular spheroid. Like cells growing on a monolayer, the avascular spheroid will only grow from oxygen and nutrients (from growth factors of the cell media) through diffusion instead of a blood supply. For a tumor spheroid, cells interact by adhering to each other and continue its growth. The outer cells of the spheroid will proliferate while the interior cells die to form a necrotic core due to a lack of nutrients. The distance oxygen and nutrients will usually travel is approximately 100 μm before being absorbed by cells, limiting the size of an avascular tumor. For the mathematical models, the tumors are limited to 500 μm to 2000 μm [20].

Multicellular spheroid models are developed *in vitro* to observe its interaction with the environment and the cell-cell interaction of the spheroid [7], [8], [9], [10], [11], [12]. Although it's usually vascular tumors that demonstrate irregular shapes, avascular spheroids begin to show different morphologies as well [4].

Metastasis can be monitored using mathematical models to observe when tumors begin to bud and branch out from a typical avascular spheroid shape [5].

Early continuum models [13], [14] were developed for tumor growth for the diffusion of nutrients. Other studies take into account conditions of a tumor for *in vivo*, such as immune response [15], mitotic inhibitor [15], [38], apoptosis [16], and growth stability [17]. The important part of a continuum model is also to observe the boundary [39], [40], identified by our mathematical equations. The boundary may be either expanding or reached its estimated maximum diameter. Morphological stability is identified by the tumor boundary [41], [42].

Computer simulations of tumor growth demonstrate how the continuum tumor model works [18]. Linear analyses and spherical geometries are limited, requiring a nonlinear model. A complex tumor has morphologies that are taken into account by an improved continuum tumor model. Through the study for computer models, tumor evolution is described by dimensionless parameters. These parameters are related to mitosis rate, apoptosis rate, cell mobility, and cell adhesion, which will be discussed further on through mathematical equations relating to the tumor model. For avascular tumors, these parameters govern the morphology of the

tumor, which is an advantage of the continuum model. At a certain point, when these parameters are scaled, the mathematical model is able to differentiate noninvasive tumor growth to unstable, infiltrative growth [18]. This suggests that the parameters used for the model to identify the morphology can also be used to identify its state of invasion. While normal spheroid tumors are limited to a certain size and potential infiltration, morphological instability increases the chance for invasion without angiogenesis. More oxygen and nutrients are also supplied to aid a tumor's invasion by increasing surface area from budding and branching cells of the spheroid. Instability would lead to complex shapes from spheroid budding which would have branches of cells with high nutrient diffusion and higher cell proliferation. This has been observed when tumors are able to bypass limits from diffusion without angiogenesis in avascular tumors [19], [20].

B. Cell Culture

MiaPaca2 cells were used to test cell growth for pancreatic cancer cells. The cells were cultured using DMEM (Dulbecco's Modified Eagle Media; 10% FBS, 1% L-glutamine) cell media. 6-well plates were seeded with MiaPaca2 cells. Each well was plated with 30,000 cells in 2.5mL of the cell/media mix (1,200 cells/mL). 24 wells were filled, totaling four 6-well plates. The well plates were placed into the incubator (37°C, humidified 17% CO₂) for 24 hours to allow cells to attach and grow on the wells.

C. Trypan Blue Staining and Cell Counting

After 24 hours, the media was aspirated from the first four wells and 1mL of PBS was added to the wells to wash the bottom. PBS was aspirated and added two more times to complete the wash. After the third wash and aspiration, 0.5mL of trypsin was added to the four wells and placed back in the incubator for approximately five minutes to detach the cells from the bottom. A pipette was used to evenly mix the detached cells into the media of the wells. 100mL was then taken from each well and pipetted into individual centrifuge capsules. 100mL of trypan blue was added to the capsules, diluting it by a factor of two. Using a hemocytometer, the cell counts of each capsule were counted, giving four cell counts (n=4), counting the living cells (white) and dead cells (blue). This was repeated at 48hr, 60hr, and 72hr intervals, counting cells from four wells each time (n=4).

D. Mathematical Model Setup

Following the design of a continuum model [18], it's assumed that the cell density of the proliferating cells is constant. Therefore, mass changes correspond to volume changes. Defining u to be the cell velocity, volume change is:

$$\nabla \cdot \mathbf{u} = \lambda_p \tag{1}$$

where λ_p is the cell-proliferation rate, defined by:

$$\lambda_p = bn - \lambda_A \tag{2}$$

where n denotes the concentration of a cell substrate (e.g. oxygen or glucose). λ_p corresponds to proliferation through mitosis while λ_A is the rate of volume loss due to apoptosis (programmed cell death). Here, λ_A is the rate of apoptosis and b is a measure of mitosis.

Since the rate of diffusion of oxygen and nutrients is much faster (e.g. $\sim 1 \text{ min}^{-1}$) than the rate of cell proliferation (e.g. $\sim 1 \text{ day}^{-1}$), the substrate may be regarded to be in a steady state for a given tumor morphology (e.g. [21, 18, 22, 14]). This gives:

$$0 = D\nabla^2 n + \Gamma \quad (3)$$

where Γ is the rate at which nutrient is added to the tumor, described by:

$$\Gamma = \lambda_B(n_B - n) - \lambda n \quad (4)$$

Here, λ_B is the blood-tissue transfer rate of nutrient, n_B is the concentration of nutrient in the blood and λ is the rate of consumption of nutrient by the tumor cells. λn describes nutrient uptake by the tumor cells. It is subtracted from the source of nutrient of the vasculature to give the rate of nutrient given. In this simplified model, the vasculature is assumed to be uniform, and vascular growth is associated with a bulk source of oxygen and nutrients. Growth is limited by the diffusion of the cell substrates according to this model.

To determine the cell velocity, Darcy's law may be used as the constitutive assumption [21], [18], [22], [13]:

$$\mathbf{u} = -\mu \nabla P \quad (5)$$

where P is the oncotic (solid) pressure and μ is a mobility that reflects the combined effects of cell–cell and cell–matrix adhesion. Alternatively, the velocity may be determined using the Stokes equations [23], [24], [25], [26] or the Darcy-Stokes (Brinkman) equations [27]. Models of viscoelasticity [28], elastoviscoplasticity [29] and soft tissue may also be used.

The boundary conditions of the tumor [18] may be set up by:

$$(n) = n^\infty \quad (6)$$

$$(P) = \gamma \kappa \quad (7)$$

where the pressure boundary condition (7) reflects the influence of cell–cell adhesion through the parameter γ and κ . Together, these two terms make the local total curvature. For equation (6), assume n^∞ is constant so that outside the tumor, the nutrient is uniform. Nutrient inhomogeneity in the tumor microenvironment in 2D has been considered [30, 20, 31, 32, 27] and more recently in 3D [33], [34], [35].

The normal velocity of the tumor boundary [21], [18], [22], [13] is:

$$V = -\mu n \cdot (\nabla P) \quad (8)$$

Following [21], [18], [22], [13] and others, assume that λ , λ_A , λ_B , n_B , and b are uniform. Following [18], denote

$$\lambda_M = b n^\infty \quad (9)$$

to be the characteristic mitosis rate,

$$\lambda_R = \mu \gamma L_D^{-3} \quad (10)$$

to be the intrinsic relaxation time scale, and

$$B = \frac{nB\lambda_B}{n^\infty(\lambda_B + \lambda)} \quad (11)$$

to be a measure of the extent of vascularization. Introducing the non-dimensional length scale $L_D = D^{1/2} (\lambda_B + \lambda)^{-1/2}$, and time scale λ_R^{-1} , a modified concentration \mathfrak{l} and pressure p can be defined [18]:

$$n = n^\infty(1 - (1 - B)(1 - \mathfrak{l})) \quad (12)$$

$$P = \left(\frac{Y}{LD}\right) * (p + (1 - \mathfrak{l})G) + \frac{AGx^2}{2d} \quad (13)$$

where G and A [18] measure the relative strength of cell–cell and cell–matrix adhesion and apoptosis, respectively:

$$G = (\lambda_M/\lambda_R) * (1 - B) \quad (14)$$

$$A = (\lambda_A/\lambda_M - B)/(1 - B) \quad (15)$$

Boundary equations for \mathfrak{l} and p can be obtained:

$$(\mathfrak{l}) = 1 \quad (16)$$

$$(p) = \kappa - AG(x^2)/2d \quad (17)$$

in a d -dimensional tumor ($d = 2, 3$). The non-dimensional normal velocity of the tumor [18] is:

$$V = -n \cdot (\nabla p) + Gn \cdot (\nabla \mathfrak{l}) - \frac{AGnx}{2d} \quad (18)$$

A study of spherically symmetric tumor growth provides insight into the regimes of growth described by the model [21], [18], [36]. In this case, the PDEs reduce to

ODEs in the polar coordinate r . From equation (18) the evolution equation for the tumor radius R [18] is:

$$\frac{dR}{dt} = V = -AG \frac{R}{d} + G, \quad \begin{cases} \frac{I_1(R)}{I_0(R)} & d = 2 \\ \frac{1}{\tanh(R)} - \frac{1}{R} & d = 3 \end{cases} \quad (19)$$

For a radially symmetric tumor, $|G|$ rescales time. In all dimensions, unbounded growth ($R \rightarrow \infty$) occurs if and only if AG is much greater than 0. Three regimes of growth are identified [18], and the behavior is qualitatively unaffected by the number of dimensions d .

(1) Low vascularization: G is much greater than 0 and A greater than 0 ($B < \frac{\lambda_A}{\lambda_M}$).

Note that the special case of avascular growth ($B = 0$) belongs to this regime. The evolution always leads to a stationary state R_∞ (if $A > 1$, then $R_\infty = 0$). This behavior is in agreement with experimental observations of in vitro diffusional growth [14] of avascular spheroids to a dormant steady state [9], [10]. In the experiments, however, tumors always develop a necrotic core that further stabilizes their growth [37].

(2) Moderate vascularization: G is much greater than 0 and A is greater than 0, where $1 > B$ (which is much greater than $\frac{\lambda_A}{\lambda_M}$). Unbounded growth occurs from any initial radius $R_0 > 0$. The growth tends to be exponential for $A < 0$ with velocity V approaching $\frac{-AGR}{d}$, as R approaches ∞ , and to be linear for $A = 0$ with velocity V approaching G as R approaches ∞ .

(3) High vascularization: $G < 0$ (where $B > 1$). For $A > 0$, growth ($V > 0$) may occur, depending on the initial radius, and is always unbounded; for $A < 0$ (for which cell apoptosis is dominant: $\frac{\lambda_A}{\lambda_M} > B$), the evolution is always to the only stationary solution $R_\infty = 0$. This stationary solution may also be achieved for $A > 0$. The stationary radius R_∞ is independent of G , and is a solution of $V = 0$ with V from equation (19).

Mass growth of a spheroid tumor can be monitored by observing the expansion of its radius over a period of time. The growth and shape of spheroids grown *in vitro* were governed by specific variables [1]: diffusion length L , the ratio of cell death rate to cell mitosis rate A , and the ratio of cell mitosis rate to relaxation rate G .

The evolving growth of a spheroid [1] can be represented as:

$$\frac{dR}{dt} = -A \left(\frac{R}{3}\right) + \frac{1}{\tanh(R)} - \frac{1}{R} \quad (20)$$

Where R is the radius of a tumor, and A is the cell death to cell proliferation ratio.

The ratio for A can be shown as:

$$A = \frac{\lambda_D}{\lambda_M} \quad (21)$$

As a tumor cell continues to grow, its growth begins to plateau until its radius becomes near constant when it doesn't have a vascular source. Its growth was only governed by the nutrients and oxygen that can diffuse through the tumor of length L [2]. From Equation 1, and setting the change of R as zero at steady state [2], the new equation is:

$$A = \frac{3}{R^2 \sinh(R)} (R \cosh(R) - \sinh(R) - R) \quad (22)$$

The radius of avascular tumors usually span a radius of 500 μm to 2000 μm . Using these parameters, the death rate to mitosis rate A can be estimated.

III. Data and Results

A chart was made using the number of cells for 24hr, 48hr, 60hr, and 72hr times.

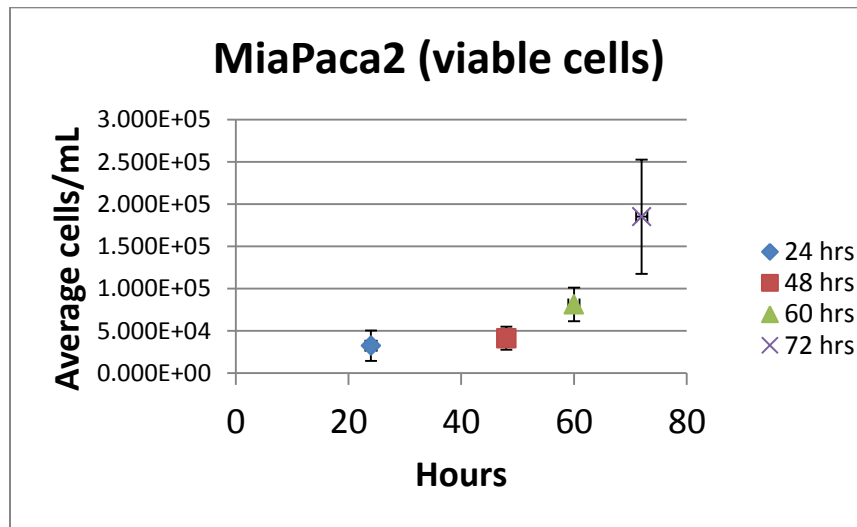


Figure 1. Living cells were monitored using trypan blue at time intervals 24hr, 48hr, 60hr, and 72hr.

From the initial slope from the chart of cancer cell growth, shown in Figure 1, the mitosis rate (λ_M) can be calculated. From the chart, λ_M was approximately 3638.4.

The cell death rate can thus be calculated by knowing A .

The radius of avascular tumors usually span a radius of 500 μm to 2000 μm . Using these parameters, the death rate to mitosis rate A can be estimated, as seen in

Figure 2.

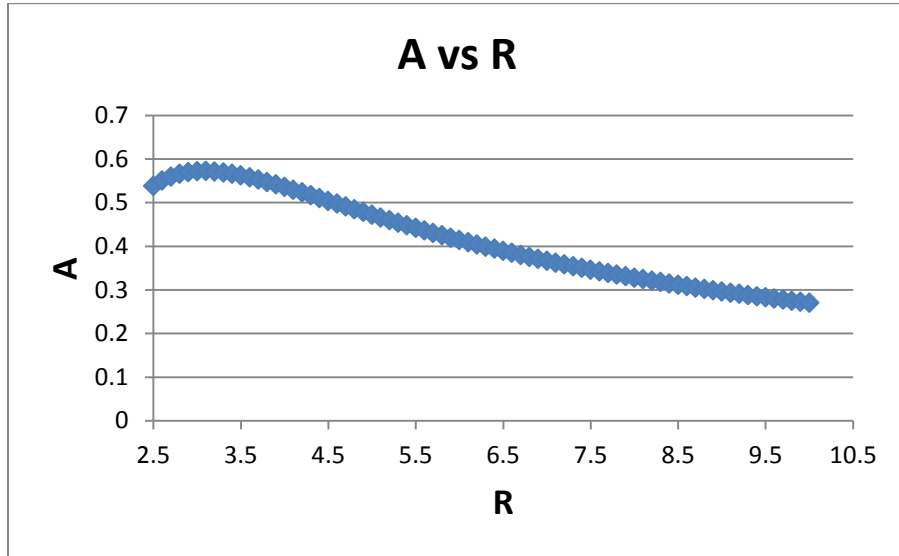


Figure 2. Relation of death variable, A, and radius of tumor, R, over a 500um to 2000um range (setting L=100um, and dividing the actual radius by L, gives a dimensionless range of 2.5 to 10).

From Figure 2, A ranges from:

$$0.27 < A < 0.57$$

Morphologically stable tumors stay within the definition of G . G regulates a stability between mitosis (mass growth) and cell death (destruction of mass). Cell growth from Figure 2, then, must remain morphologically stable [1], as defined by:

$$A = \frac{54}{G} * \frac{1}{R^3} - \frac{3}{4} + \frac{3}{4} \left(\frac{7}{R} + \frac{I_{11} * R}{I_9 * R} \right) \left(\frac{1}{\tanh(R)} - \frac{1}{R} \right) \quad (23)$$

Where $I_{11/2}$ and $I_{9/2}$ were Bessel functions, and G (the ratio of cell mitosis rate to mechanical relaxation rate) was identified [1],[2] by:

$$G = \frac{\lambda_M}{\lambda_R} \quad (24)$$

Using the range of A (0.27 to 0.57) found from Figure 2, the boundaries of G were found through Equation 23 and plotted, as seen in Figure 3. The values of A used were 0.27 (lowest value), 0.42 (mid-range), and 0.57 (highest value).

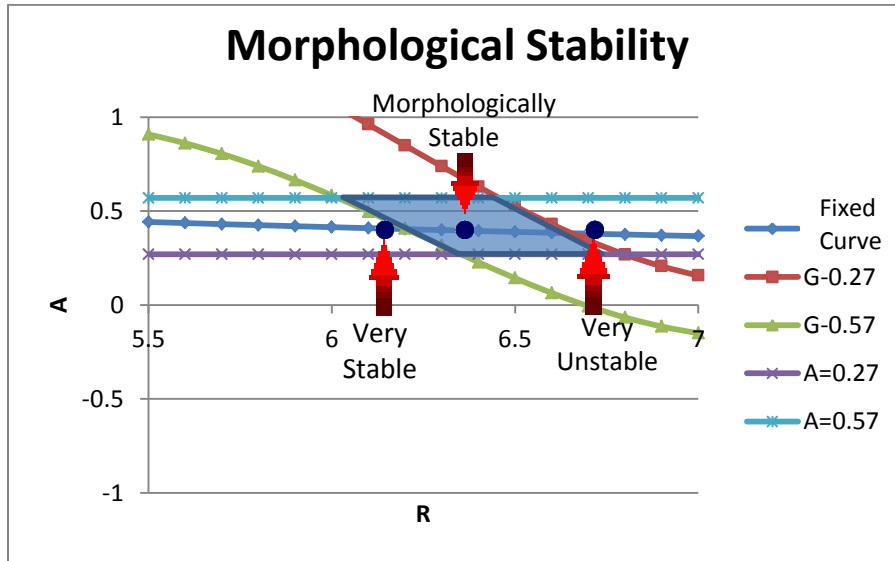


Figure 3. Using the boundaries of A (0.27 and 0.57), the area between $G=0.27$ and $G=0.57$ was morphologically stable for tumor spheroids.

IV. Discussion

From Figure 3, the stability of the tumor mass is monitored. Following the stationary curve in the center, any tumor in the shaded area and to the left is morphologically stable. As the radius increases along the stationary curve (when $\frac{dR}{dt} = 0$), moving past the shaded area to the right, the tumor becomes unstable.

The increase of the radius as its growth plateaus is an indication that the tumor is developing a small G ratio and a larger relaxation rate. This instability was based on the spheroid shape of the tumor. As instability increases, the cell adhesion forces that keep the tumor together deteriorate and the tumor begins to bud and expand. Budding parts of the tumor mark the invasiveness of a tumor, increasing the surface area of the tumor for more nutrients and oxygen. As the tumor develops a large G ratio, identifying a large mitosis rate, this may indicate micrometastasis. Small areas continue to lose cell adhesion as instability (based on G) increases [33].

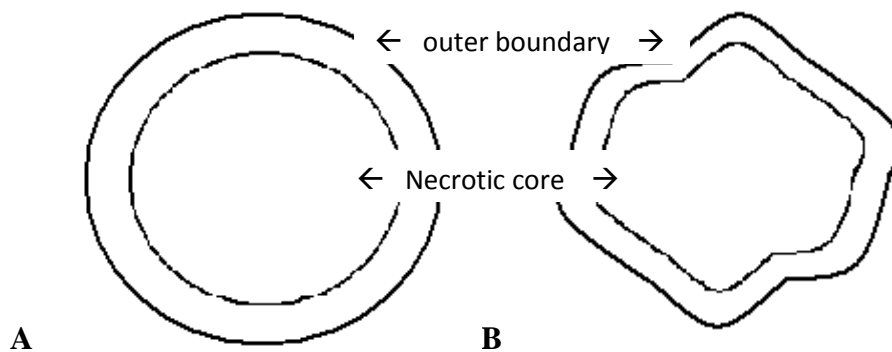


Figure 4. Mathematical models of morphological states. Stable spheroids (A) maintain a spherical shape when it is limited by size in its avascular state. When spheroids become unstable (B), the surface begins to branch and invade surrounding tissue. The forces that keep the tumor together lose effect as the tumor is predicted to metastasize.

When analyzing the progression of a tumor, G may be an important identifier to tumors that were beginning to metastasize in patients. This work uses cell growth data, as demonstrated from the *in vitro*, to estimate the stability. A dimensionless unit G was estimated by $\frac{6}{R}$. In cases where R can't be accurately determined,

morphological stability can determine A . Tumor progression may be monitored by observing the cell death rate to the cell mitosis rate. Plotting a stationary curve to Figure 3 and observing A , as was done above using the data from the MiaPaca 2 cells in Figure 1, can give observations as to when the tumor shifts to the right of the shaded area. When A decreases to a point where cell death was significantly less than cell mitosis, the tumor becomes morphologically unstable. Observations from *in vitro* can identify beginning of metastasis using mathematical models. When performing *in vitro* experiments with a patient's tumor cells, the values of A will change, consequently changing the area of the shaded region as well. The changing graph according to a patient's tumor growth and the parameter A will indicate what stage a patient is currently.

Morphological instability is an indicator of metastasis, and observing parameters through mathematical models allow practitioners to monitor tumor activity.

Metastasis was previously thought to derive from malignant tumors [6], but newer reconsiderations are being tested for a tumor's metastatic ability. Models that demonstrate branching represent *in vivo* tumors that are invading surrounding tissue. The important concept to take away from this is that branching areas of tumor cells have the potential to absorb more nutrients and oxygen, and could eventually "pinch off" of the original tumor.

The aim of these mathematical models and cells grown *in vitro* is to represent *in vivo* tumor growth. Understanding growth of 3D tumors will benefit

diagnosticians to make decisions on the best course of treatment for each patient. In the future, mathematical models can aid research to counter tumor progression. Pancreatic cancer is a particularly aggressive cell line that can be monitored morphologically to understand and limit its invasive nature. The aggressive nature of pancreatic cancer leads to a high mortality rate in patients. Understanding the tumor growth of these cells would not only act as a beneficial model in designing drug deliveries and therapies, but alert diagnosticians when a tumor is approaching malignant condition. With this goal, mathematical models can be designed to predict the 3D nature of cancerous tumors, as well as its growth and progression toward metastasis.

References

1. Frieboes HB, Zheng X, Sun C-H. Feb 2006. "An Integrated Computational/Experimental Model of Tumor Invasion" *Cancer Res* 2006; 66:1597-1604.
2. Lowengrub JS, Frieboes HB, Jin F, Chuang Y-L, Li X, Macklin P, Wiseand SM, Cristini V. Dec 2009. "Nonlinear modelling of cancer: bridging the gap between cells and tumours" *Online at stacks.iop.org/Non/23/R1..*
3. Jiang Y, Pjesivac-Grbovic J, Cantrell C, Freyer J. "A Multiscale Model for Avascular Tumor Growth." *Biophysical Journal* 89.6 (2005): 3884-894.
4. Enmon RM, Jr., O'Connor KC, Lacks DJ, Schwartz DK, Dotson RS. "Dynamics of spheroid self-assembly in liquid-overlay culture of DU 145 human prostate cancer cells" *Biotechnol Bioeng* 2001;72:579-91.
5. Byrne H, Matthews P. "Asymmetric growth of models of avascular solid tumours: exploiting symmetries" *IMA J Math Appl Med Biol* 2002;19:1-29.
6. Podsypanina K, Du YC, Jechlinger M, Beverly LJ, Hambardzumyan D, Varmus H (September 2008). "Seeding and Propagation of Untransformed Mouse Mammary Cells in the Lung". *Science* 321 (5897): 1841-4. doi:10.1126/science.1161621. PMC 2694414. PMID 18755941.
7. Kim JB. 2005. "Three-dimensional tissue culture models in cancer biology" *J. Biomol. Screening*.
8. Kunz-Schughart LA, Freyer JP, Hofstaedter F and Ebner R. 2004. "The use of 3-d cultures for high-throughput screening: the multicellular spheroid model" *J. Biomol. Screening*.
9. Mueller-Klieser W. 1987. "Multicellular spheroids: a review on cellular aggregates in cancer research" *J. Cancer Res. Clin. Oncol*.
10. Sutherland RM. 1988. "Cell and environment interactions in tumor microregions: the multicell spheroid model" *Science*.
11. Sutherland RM, Carlsson J, Durand RE and Yuhua J. 1981. "Spheroids in cancer research" *Cancer Res*.

12. Walles T, Weimer M, Linke K, Michaelis J and Mertsching H. 2007. "The potential of bioartificial tissues in oncology research and treatment" *Onkologie*.
13. Greenspan HP. 1972. "Models for the growth of a solid tumor by diffusion" *Stud. Appl. Math.*
14. Greenspan HP. 1976. "On the growth and stability of cell cultures and solid tumors" *J. Theor. Biol.*
15. Adam JA. 1996. "General aspects of modeling tumor growth and the immune response" *A Survey of Models on Tumor Immune Systems Dynamics ed J Adam and N Bellomo pp 15–87*.
16. McElwain DLS and Morris LE. 1978. "Apoptosis as a volume loss mechanism in mathematical models of solid tumor growth" *Math. Biosci.*
17. Shymko RM and Glass L. 1976. "Cellular and geometric control of tissue growth and mitotic instability" *J. Theor. Biol.*
18. Cristini V, Lowengrub JS and Nie Q. 2003. "Nonlinear simulation of tumor growth" *J. Math. Biol.*
19. Debnath J, Mills KR, Collins NL, Reginato MJ, Muthuswamy SK and Brugge JS. 2002. "The role of apoptosis in creating and maintaining luminal space within normal and oncogene-expressing mammary acini" *Cell*.
20. Frieboes HB, Zheng X, Sun C-H, Tromberg BJ, Gatenby R and Cristini V. 2006. "An integrated computational/experimental model of tumor invasion" *Cancer Res*.
21. Byrne HM and Chaplain MAJ. 1995. "Growth of nonnecrotic tumors in the presence and absence of inhibitors" *Math. Biosci.*
22. Friedman A and Reitich F. 1999. "Analysis of a mathematical model for the growth of tumors" *J. Math. Biol.*
23. Franks SJ, Byrne HM, King JR, Underwood JCE and Lewis CE. 2003. "Modeling the early growth of ductal carcinoma in situ of the breast" *J. Math. Biol.*
24. Franks SJ and King JR. 2003. "Interactions between a uniformly proliferating tumor and its surrounding uniform material properties" *Math. Med. Biol.*

25. Friedman A and Hu B. 2007. "Bifurcation from stability to instability for a free boundary problem modeling tumor growth by stokes equation" *J. Math. Anal. Appl.*
26. Wu J and Cui S. 2009. "Asymptotic behavior of solutions of a free boundary problem modeling the growth of tumors with stokes equations" *Discrete Contin. Dyn. Syst.*
27. Zheng X, Wise SM and Cristini V. 2005. "Nonlinear simulation of tumor necrosis, neovascularization and tissue invasion via an adaptive finite-element/level-set method" *Bull. Math. Biol.*
28. MacArthur BD and Please CP. 2004. "Residual stress generation and necrosis formation in multi-cell tumour spheroids" *J. Math. Biol.*
29. Ambrosi D, Duperray A, Peschetola V and Verdier C. 2009. "Traction patterns of tumor cells" *J. Math. Biol.*
30. Cristini V, Frieboes HB, Gatenby R, Caserta S, Ferrari M and Sinek J. 2005. "Morphologic instability and cancer invasion" *Clin. Cancer Res.*
31. Macklin P and Lowengrub JS. 2007. "Nonlinear simulation of the effect of microenvironment on tumor growth" *J. Theor. Biol.*
32. Macklin P and Lowengrub JS. 2008. "A new ghost cell/level set method for moving boundary problems: Application to tumor growth" *J. Sci. Comput.* 3.
33. Frieboes H B, Lowengrub J S, Wise S M, Zheng X, Macklin P, Bearer E L and Cristini V 2007. "Computer simulation of glioma growth and morphology" *NeuroImage.*
34. Sanga S, Frieboes HB, Zheng X, Gatenby R, Bearer EL and Cristini V. 2007. "Predictive oncology: a review of multidisciplinary, multiscale in silico modeling linking phenotype, morphology and growth" *NeuroImage.*
35. Wise SM, Lowengrub JS, Frieboes HB and Cristini V. 2008. "Three-dimensional multispecies nonlinear tumor growth: I. Model and numerical method" *J. Theor. Biol.*

36. Li X, Cristini V, Nie Q and Lowengrub JS. 2007. "Nonlinear three-dimensional simulation of solid tumor growth" *Discrete Dyn. Contin. Dyn. Syst. B*.
37. Byrne HM and Chaplain MAJ. 1996. "Growth of necrotic tumors in the presence and absence of inhibitors" *Math. Biosci.*
38. Cui S. 2002. "Analysis of a mathematical model for the growth of tumors under the action of external inhibitors" *J. Math. Biol.*
39. Cui S. 2007. "Well-posedness of a multidimensional free boundary problem modelling the growth of nonnecrotic tumors" *J. Funct. Anal.*
40. Cui S and Escher J. 2008. "Asymptotic behaviour of solutions of a multidimensional moving boundary problem modeling tumor growth" *Commun. Partial Diff. Eqns.*
41. Friedman A and Hu B. 2005. "Asymptotic stability for a free boundary problem arising in a tumor model" *J. Diff. Eqns.*
42. Guiot C, Del Santo PP and Deisboeck TS. 2007. "Morphological instability and cancer invasion: a 'splashing water drop' analogy" *Theor. Biol. Med. Model.*
43. Tao Y and Chen M. 2006. "An elliptic-hyperbolic free boundary problem modeling cancer therapy" *Nonlinearity*
44. Tao Y, Yoshida N and Guo Q. 2004. "Nonlinear analysis of a model of vascular tumour growth and treatment" *Nonlinearity*.
45. Wu J and Cui S. 2009. "Asymptotic behavior of solutions of a free boundary problem modeling the growth of tumors with stokes equations" *Discrete Contin. Dyn. Syst.*